The increase in the FWHM of these peaks can be attributed to the presence of higher disorder effects that would be related to a worsening of the crystalline quality at the back region of the layers. This agrees with the cross-section SEM image of the samples, which shows the presence of a region close to the back interface with smaller crystal grains, as can be seen in Figure 4. On the other hand, the red shift of the peak could be due to stress induced effects, which could indicate an increasing tensile stress component in this region. However, chemical induced effects – likely related to a higher content of vacancies at this region- could also lead to the observed red shift of the peaks. Further measurements are required to clarify this issue.

Finally, it is interesting to remark the presence of the peak characteristic of Cu_ySe in the spectra from sample with x = 0.92. As shown in Figure 3, the spectrum measured on the back surface has even a higher intensity of this mode. This is likely related to the inclusion of a Cu_ySe grain in the submicronic light spot. These spectra corroborate the occurrence of this binary phase inside the layers from Cu-poor samples with composition close to stoichiometry.

CONCLUSIONS

The Raman scattering analysis of Cu-poor CIS polycrystalline layers corroborates the presence of both OVC and CuAu CIS phases in the ranges of compositions corresponding to $x \leq 0.82$ (OVC) and $x \leq 0.66$ (CuAu-CIS). The in-depth resolved analysis of the layers with lower Cu content ($x \leq 0.57$) shows a strong inhibition of the Raman peak of the CH-CIS phase at the back region of the layers. This is likely related to an enhanced formation at the region close to the back interface with the Mo coated substrate of both the OVC and metastable CuAu ordered phases.

On the other hand, for values of $x \geq 0.66$, the spectra are dominated by the A_1 peak of CH-CIS. The comparison of the spectra directly measured on the front and back surface of the layers (after removal of the absorber from the Mo coated substrate) suggests a worsening of the crystalline quality in the region close to the CIS/Mo interface. For the samples with lower Cu contents ($x < 0.66$), this is also accompanied by an increase in the spectral contribution of the OVC phase, suggesting an increase in the occurrence of this phase at the CIS/Mo interface region.

REFERENCES

1. D. Schmid et al., J. Appl. Phys. **73** 2902 (1993)
2. J. Álvarez-García et al., Phys. Rev. B **71** 054303 (2005)
3. Ch.-M. Xu et al., Semicond. Sci. Technol. **19** 1201 (2004)
4. L. Calvo-Barrio et al., Vacuum **63** 315 (2001)
5. C. Rincón et al., Appl. Phys. Lett. **73** 441 (1998)
6. G. Morell et al., Appl. Phys. Lett. **69** 987 (1996)
7. B.J. Stanbery et al., J. Appl. Phys. **91** 3598 (2002)
8. B. Barcones, PhD Thesis, Universitat de Barcelona, 2007
9. V. Izquierdo-Roca et al., Phys. Status Solidi A **206** 1001 (2009)
10. W. Witte et al., Thin Solid Films **517** 867 (2008)

Mater. Res. Soc. Symp. Proc. Vol. 1165 © 2009 Materials Research Society 1165-M05-17

A Rapid Screening Method for Investigating the Effect of Processing Parameters on CdTe/CdS Solar Cell Performance

Mohammed Al Turkestani[1*], Ken Durose[1], Ben Wakeling[2], David Lane[2], Stuart Irvine[3] and Vincent Barrioz[3]

[1]Department of Physics, Durham University, The Science Laboratories, South Rd, Durham, DH1 3LE, UK

[2] Centre for Materials Science and Engineering, Dept of Materials and Medical Sciences, Cranfield University, Shrivenham, Swindon, SN6 8LA, UK

[3] Centre of Solar Energy Research, Glyndŵr University/ OpTIC Technium, St Asaph Business Park, St Asaph, LL17 OJD, UK

ABSTRACT

A rapid screening method is reported in which material processing parameters are investigated as a function of the CdTe absorber thickness in CdTe/CdS solar cells. The technique has been used to investigate i) the optimum absorber thickness for $CdCl_2$ processing at 380°C for 10 mins, and ii) the effect on device performance of post-growth annealing of CdS layer with H_2, N_2, and O_2. It was found that the optimum thickness of CdTe compatible with the processing conditions was ~3μm. The device results were independent of the post-growth treatment of the CdS for the conditions investigated here. The bevel method allowed for ~30 data points to be obtained from each sample, giving a significant advantage over conventional experimental methods.

INTRODUCTION

Contrary to the way in which silicon based microelectronic devices and many optoelectronic devices are designed and fabricated, the development of thin film polycrystalline devices has been largely conducted by process optimisation. In the case of the CdTe/CdS/TCO/glass solar cell, the contacting, $CdCl_2$ processing, interdiffusion, grain boundaries, impurities (including oxides) are all thought to interact. The number of experiments required for complete optimisation is therefore very large.

As a result there is a need for rapid screening methodologies with the aim of reducing the number of samples required in order to fully explore a region of processing parameter space. Such methods may find application both in existing technologies, and for new and emerging thin film systems.

One particular embodiment of rapid screening is the use of a wedge-shaped sample in order to simultaneously explore a range of film thicknesses in a single processing run. In this work the use of a bevelling method to produce CdTe/CdS samples having a range of CdTe thicknesses has been explored. The CdTe thickness is therefore selected to be the primary variable. Two variations of this methodology have been explored: screening process A, in which the sample was bevelled prior to $CdCl_2$ processing, and screening process B, in which the bevelling followed the $CdCl_2$ treatment step. Both methodologies were applied to each of three kinds of cells in which the CdS had itself been processed differently i.e. treated with N_2, H_2 and O_2 (as described in the Experimental section).

In a preliminary study using this same method, fully clear results were not obtained and that was attributed to non-uniformity in the plates used for that work [1]. In this work that limitation was addressed. With the improvements used here, it was demonstrated that the method is capable of identifying an optimum thickness of CdTe appropriate to a given set of conditions (i.e. temperature and duration) for $CdCl_2$ processing.

EXPERIMENT

The samples studied had a structure of CdTe (~9 μm)/CdS (~150 nm)/TCO/glass. For the bevelling experiments it was essential to obtain uniform sample plates. Preliminary experiments established that suitable growth and processing conditions were as follows: The TCO/glass was Pilkington TEC15. CdS was grown by chemical bath deposition at Cranfield University [2]. CdTe was grown using close space sublimation under 2 torr of O_2 and a substrate temperature of 520°C. The sequence of the screening and device fabrication steps used is summarised in table I and is now described here in detail. For this rapid screening work, the primary variable was the CdTe thickness. Bevel etching of the CdTe layers of the cells was achieved by controlled immersion into Br_2 (4.5% by volume): methanol (25.5%): ethylene glycol (70%). This step was performed using a U-tube with a flexible tubular link, the height of one of the tubes being controlled by a slow motor. In this way, samples were obtained in which the CdTe had a ramp of thickness values, ranging from ~ 9 μm (the as-grown value) to zero, over a distance of ~2 cm.

Table I: Processing steps of all samples used in this study showing the differences between screening process A and B and highlighting the processing variations used for the CdS

Step	Description	
1	CdS deposition: by CBD	
2	Post-growth CdS annealing: 3 torr of either i) N_2, ii) H_2 or iii) O_2 at a nominal temperature of 400 °C for 5 mins (Secondary variable – further details in text)	
3	CdTe: CSS in 2 torr of O_2	
	Post-growth processing	
	Screening process A	Screening process B
4	Bevel CdTe (Primary variable)	50 nm of $CdCl_2$, annealed at 380 °C for 25 mins
5	50 nm of $CdCl_2$, annealed at 380 °C for 10 mins	Bevel CdTe (Primary variable)
6	NP etch and matrix of dot contacts	NP etch and matrix of dot contacts

There were two variations of the screening methodology. In process A, the bevelling was done first and followed by the $CdCl_2$ annealing. In process B, these two steps were reversed, as shown in table I. In this study the secondary variable was the post-growth annealing of the CdS in either N_2, H_2 or O_2 prior to deposition of the CdTe. Annealing was performed under pure flowing gas (50 sccm) or at 3 torr for 5 mins. The procedure was to set the substrate temperature at 400°C with the sample in vacuum. Upon introduction of the gas flow there was a rapid drop in temperature to as low as 270°C, and then recovering to 350°C at the end of a run.

Cells which had been processed and bevelled (both A and B types) were contacted by i) NP etching for 10 seconds in a solution of H_3PO_4 (70% by volume) : H_2O (29%) : HNO_3 (1%)[3]

followed by ii) evaporation of a matrix of 2 mm diameter gold dot contacts. The dot contacts were applied in a 4×4 mm square matrix, there being 25-36 dots on each ~ 25×25 mm sample. In order to maximize the number of CdTe thickness values investigated, the matrix was applied at an offset angle of ~10°. No scribing was used prior to J-V measurement. Local values of thicknesses were however measured by scribing and step profiling with an Ambios XP 200 profiler. Roughness was measured using the same instrument. Images were also obtained by SEM. J-V curves were recorded under approximate AM 1.5 (1000 W/m^2) conditions. Light biased (1 sun) EQE curves were obtained using a Bentham system at Glyndŵr University.

RESULTS

Screening Process A (CdTe Bevel Etch Followed by $CdCl_2$ Treatment)

Figure 1 shows the device characterization outcomes for cells that were subjected to the three different kinds of CdS processing and screening process A as shown in table I. The values of η, FF, J_{sc} and V_{oc} (efficiency, fill factor, short circuit current density and open circuit voltage) are shown as a function of the thickness of CdTe. The efficiency curves each show a maximum response for CdTe thickness of ~2.5-3 μm, irrespective of the treatment applied to the CdS. Examination of figure 1 indicates that these curves are dominated by the behaviour of J_{sc}, which peaks at ~3 μm also. For values >3 μm, η decreases, and this is the general behaviour for FF, J_{sc} and V_{oc} also. EQE measurements of both high performing parts of the cells (~3 μm), and lower performing parts (higher thicknesses) were made, with typical curves being shown in figure 2. The response for the optimum device shows normal behaviour, whereas that for the thick device has a curve characteristic of a buried junction.

A minor feature of the behaviour of the curves, i.e. their behaviour at high CdTe thicknesses values, is now described: Firstly, in this region all of the graphs show increased scatter. Examination of the roughness data (figure 3) indicates that this could be due to the increased roughness of the thicker parts of the samples. Secondly notwithstanding this scatter, there is an apparent increase in V_{oc} at high thicknesses in all samples. It may be speculated that this results from the fact that in the thicker parts of the samples there is reduced opportunity for leakage via accidental conductive paths.

Screening Process B ($CdCl_2$ treatment followed by CdTe bevel etch)

An identical set of samples to those shown in figure 1 were subjected to screening process B in which $CdCl_2$ treatment preceded the bevel-etch thinning of the CdTe (see table I). For this second set of samples, a data set somewhat similar to that shown in figure 1 was obtained, but is not shown here. Significant differences in the two data sets were observed as follows: i) the results had greater scatter in process B than for process A, ii) while all working parameters of the cells decreased with increasing CdTe thickness as before, the data showed no clear peaks, iii) contrary to the results in figure 1, differences in the influence of the processing gases were seen: while H_2 and O_2 gave efficiencies in the range 2.5 - 6%, N_2 acted to depress the efficiency to the level of 0.5 - 2.5%. There was also distinctive behaviour for high thicknesses of CdTe: i) there was roughness induced scatter (see figure 3 for the roughness data), and ii) there was further evidence of enhanced V_{oc} for these higher thicknesses.

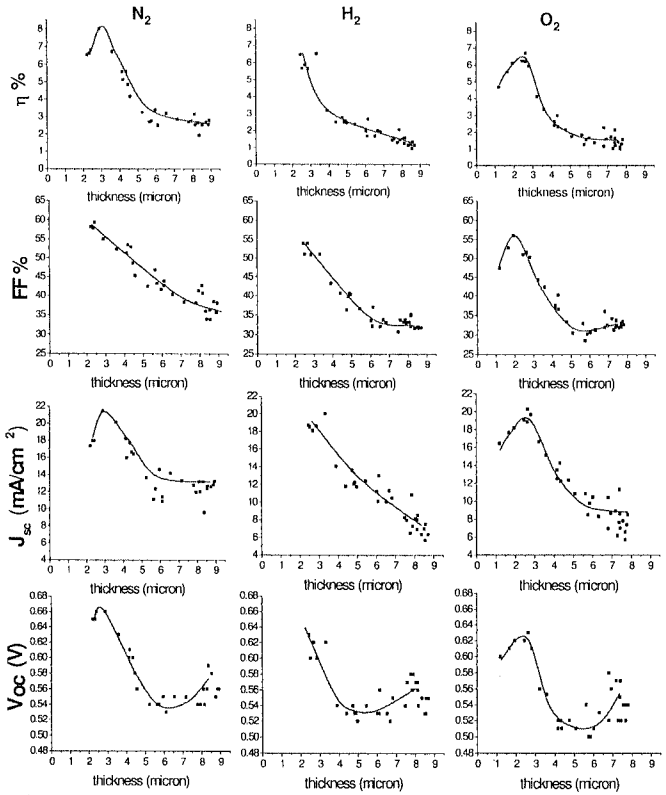

Figure 1: Device results for process A, showing all the working parameters (for samples with CdS processed under N_2, H_2 and O_2) as a function of CdTe thickness.

DISCUSSION

The clear trends in parameter variation seen in the device results as a function of CdTe thickness (figure 1) indicate that the device material and procedure were of sufficient quality in order to allow the screening method to work. There is a clear reduction in the scatter of data points obtained compared to that in the earlier preliminary work [1].

In figure 1, the most striking feature of the results is that there is a peak in efficiency for a CdTe thickness of ~ 3 μm for all of the cells tested. It may be inferred that for the $CdCl_2$ processing conditions used, 3 μm is the optimum thickness of CdTe. While the exact concentration profile resulting from this diffusion has not been measured, we might speculate that the profile is optimal for 3 μm for CdTe i.e. it generates junction position that gives the best

collection performance. It may also be inferred that for thicknesses greater than 3μm, the extent of diffusion is insufficient to form a junction with a maximum collection efficiency i.e. the cell is under processed. Moreover, for thicknesses less than 3μm, this $CdCl_2$ treatment gives over processed cells. This was explored further and it was found that the thicker parts of the cells had buried junction behaviour, while the optimum thicknesses had normal behaviour. The observation that the efficiency is dominated by J_{sc} is consistent with this.

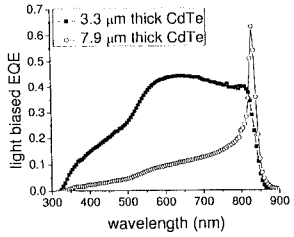

Figure 2: Light biased EQE data from dot contacts corresponding to CdTe thicknesses of 3.3 and 7.9 μm from the cell with H_2-treated CdS. The thicker sample shows the characteristics of a buried junction.

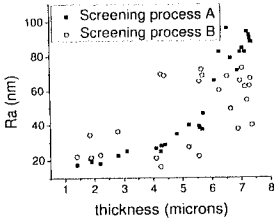

Figure 3: Development of roughness with sample thickness for CdTe bevels from processes A and B (see Table I).

Whereas there was a clear dependence of the performance of the cells on CdTe thickness (the primary variable), it is noticeable that the post growth treatment of the CdS in N_2, H_2 and O_2 (secondary variable) had little influence on the performance. Annealing of the CdS this way might be expected to have a number of direct effects on the material itself. For example, annealing in H_2 may act to form H_2S thereby increasing the population of V_S. Annealing in O_2 may promote formation of CdO. Heating may cause residual hydroxides in the CBD CdS to be converted to CdO. There are two possible explanations of the null result: i) that the temperature and duration of the annealing were insufficient to effect significant change to the material, or ii) that any annealing-induced change was eliminated by the subsequent CdTe growth. Indeed the CSS growth of CdTe was carried out at 520°C under 2 torr of O_2 over 12 mins, and it is therefore likely that those conditions, and interdiffusion during growth may have dominated the result.

For process B, the much increased scatter in the data points was accompanied by a significant increase in surface roughness, as shown in figure 3. This is considered to arise from the $CdCl_2$ treatment (annealing in air) that preceded the bevel etching in Br_2/methanol/ethelene glycol used in process B. Oxide layers on CdTe are known to inhibit etching with Br_2-based solution, as was shown to be the case for work on oxidised single crystals [4]. It is likely that local masking effects due to non-uniform coverage by oxide have lead directly to the increased roughening of samples subjected to process B. This roughness variation may be expected to lead directly to increased scatter of the data.

Contrary to the findings from process A, for process B it was found that H_2 and O_2 gave better device results than were obtained for N_2 annealing of the CdS. No immediate explanation is available for this behaviour and it should be investigated by repeat runs.

The slight increase of V_{oc} associated with high thicknesses of CdTe observed for most samples was attributed to the lower incidence of leakage paths likely in thicker absorber layers.

For both processes it was considered that any systematic effect from the bevel etching would be outweighed by the (more severe) NP etching used to form a contact on all samples.

CONCLUSIONS

A rapid screening methodology for investigating the results of thin film solar cell materials processing as a function of continuously varied absorber layer thickness has been demonstrated. The method used bevel etching of the film in order to generate ramps of thickness, and was applied to CdTe/CdS/TCO/glass solar cells. The clear trends in device performance parameters seen in figure 1 give some confidence that the device uniformity was sufficiently high for the only variable to be the CdTe thickness. Application of a standard post-growth $CdCl_2$ annealing step (380°C for 10 mins in air) to the bevelled sample plates (process A) identified an optimum thickness for the CdTe that was exactly compatible with this processing. The efficiency of devices on the plate was controlled by J_{sc}, and EQE results showed that this was itself controlled by the junction position.

The second variable investigated in this work was post-growth annealing of the CdS with N_2, H_2 and O_2. However it was shown that this annealing step had no influence on the device results for any CdTe thickness. This was attributed to the dominance of the subsequent CdTe growth ambient and conditions that acted to mask any annealing induced change.

This bevel-etch based screening method is subjected to data scatter that is controlled by surface roughness. In particular it was found that i) high thicknesses of CdTe, and ii) samples which were first $CdCl_2$ treated and then bevelled (process B) were subjected to greater data scatter than others. Polishing procedures may be devised to reduce this.

Each sample plate used in this work had 25-36 contact dots, allowing the same number of CdTe thickness values to be investigated. Hence the screening method accelerates parameter studies by a factor of ~30 i.e. one sample replaces a series of 30 conventional growth runs. Moreover since an investigation may be concluded over a smaller number of growth runs, the requirements for run-to-run reproducibility are relaxed. It may be concluded that the use of this and similar rapid screening methodologies will be of advantage in the empirical development of both new and emerging solar cell processing technologies.

REFERENCES

1. M. K. Al Turkestani and K. Durose. *A Rapid Screening Study of the Influence on Interfaces and Thickness on CdTe/CdS Solar Cells*, Conference Record of PVSAT-4, Bath, UK, 2008 pp. 105-108.
2. Udaya S. Ketipearachchi, David W. Lane, Keith D. Rogers, Jonathan D. Painter, and Michael A. Cousins, Mater. Res. Soc. Symp. Proc. 836, 161-166 (2004).
3. M. Hädrich, N. Lorenz, H. Metzner, U. Reislöhner, S. Mack, M. Gossla and W. Witthuhn, Thin Solid Films 515, 5804 (2007).
4. S. Greengrass and K Durose, unpublished work.

Mater. Res. Soc. Symp. Proc. Vol. 1165 © 2009 Materials Research Society 1165-M05-20

Influence of the Cu Content on Structural and Vibrational Properties in Polycrystalline $CuGaSe_2$ Thin Films

Wolfram Witte, Robert Kniese and Michael Powalla
Zentrum für Sonnenenergie- und Wasserstoff-Forschung Baden-Württemberg (ZSW), Industriestrasse 6, D-70565 Stuttgart, GERMANY

ABSTRACT

We studied $CuGaSe_2$ (CGS) thin films with different Cu contents by means of X-ray diffraction (XRD) and micro-Raman spectroscopy. The CGS absorbers were deposited by co-evaporation on Mo/glass substrates. We found a clear shift of the CGS Raman mode frequencies to lower values with increasing Cu/Ga ratio. This is in direct correlation with the increasing lattice constants a and c extracted from XRD patterns. Influence of stress on the obtained results can be neglected, because very small stress values below 50 MPa were determined with the $\sin^2\Psi$ method.

INTRODUCTION

$CuGaSe_2$ (CGS) thin films are a candidate for application as the top cell in tandem solar cell devices with $Cu(In,Ga)Se_2$ (CIGS) as the bottom cell. So far, the maximum achieved conversion efficiencies of CGS thin-film solar cells [1] are too low for such an application, motivating basic research on the properties of this material. One interesting characterization method is the non-destructive technique of Raman spectroscopy, a promising tool for the in-line process monitoring of CIGS films in solar cell production.

This contribution reports on the influence of the Cu content in CGS polycrystalline thin films on the Raman spectra, especially regarding changes in the frequency of the CGS modes. Lattice constants were determined from X-ray diffraction (XRD) measurements for comparison. Furthermore, the stress in the CGS films was analyzed and its influence on the Raman phonon frequencies is estimated.

EXPERIMENT

The polycrystalline CGS thin films were co-evaporated in-line on Mo-coated soda lime glass. The thickness of the glass is 3 mm and the sputtered Mo films are 0.5 µm thick. The CGS films have a thickness of 2 µm and typical growth temperatures were around 550-560 °C. We determined the final film composition of the samples by X-ray fluorescence analysis with an EDAX-Eagle µProbe equipped with a Rh tube.

XRD spectra were recorded with a Bruker D8 Discover with a parallel beam geometry in the θ-2θ scanning mode using Cu-K_α radiation. The Euler cradle was used for the stress measurements. We recorded Raman spectra with a WITec CRM 200 confocal micro-Raman system in the back-scattering geometry at room temperature. A frequency-doubled Nd:YAG